EphA2 Targeted Doxorubicin Stealth Liposomes as a Therapy System for Choroidal Neovascularization in Rats

Jia-lin Wang,[1] *Yu-ling Liu,*[*,1] *Ying Li,*[1] *Wen-bing Dai,*[2] *Zhao-ming Guo,*[2] *Zhao-hui Wang,*[2] *and Qiang Zhang*[*,2]

Purpose. To enhance drug uptake in RPE cells, improve efficacy for choroidal neovascularization (CNV), and reduce drug toxicity, an EphA2-targeted nanocarrier loaded with doxorubicin (DOX) was developed by conjugation with a homing peptide YSA.

Methods. The YSA was coupled to PEGylated lipid. Then, YSA-modified DOX stealth liposomes (YSA-SSL-DOX) were prepared and characterized. Their uptake in a human RPE cell line (ARPE-19) was evaluated. After intravitreous injection, their efficacy against CNV was assessed in a laser-induced rat model. Finally, TUNEL test and morphology observation on rat retina were conducted.

Results. The prepared YSA-SSL-DOX was approximately 110 nm in particle size, with an encapsulation efficiency of DOX more than 95%. The leakage of DOX from YSA-SSL-DOX was very slow. The expression of EphA2 on the CNV was confirmed. Both flow cytometry and confocal microscopy studies revealed that YSA-SSL-DOX could facilitate the uptake of liposomal DOX into ARPE-19 cells. Treatment with YSA-SSL-DOX (2.5 μg DOX) resulted in a significant reduction in the CNV area of rats compared with the unmodified liposomal DOX and normal saline ($P < 0.05$). No obvious toxicity of YSA-SSL-DOX on rat retina was found.

Conclusions. EphA2-targeted stealth liposomes might be an effective delivery and therapy system for angiogenesis-related diseases in the retina. (*Invest Ophthalmol Vis Sci.* 2012; 53:7348–7357) DOI:10.1167/iovs.12-9955

Choroidal neovascularization (CNV) causes severe vision loss, especially in AMD patients.[1] Recently, different kinds of antiangiogenic agents have been used in the clinic to treat CNV.[2,3] However, in order to maintain the therapeutic level of a drug in target tissues, frequent administration for an extended period of time is often required. Besides, a systemically administered drug does not reach the target tissue effectively, resulting in unwanted side effects. To solve these problems, a drug delivery system targeted to CNV is extremely significant.

Recent studies show that receptor EphA2 and its ligand ephrinA1 play a role in tumor neovascularization.[4] Besides, they are found to be related in corneal and retinal angiogenesis.[5–8] Additionally, ephrinA1 is highly expressed in embryonic but not adult vasculature.[9] These results suggest that EphA2 may be an effective target, not only for tumor angiogenesis but also for ocular neovasculatures.

A 12–amino acid peptide (YSAYPDSVPMMS) coded as YSA, which is a bioactive ephrin mimetic peptide, could selectively bind to EphA2.[10] This actually provides the opportunity to use YSA as the homing peptide in the targeted delivery of cytotoxic agents to neovasculatures formed in diseased tissues and to selectively kill related target cells.

Doxorubicin (DOX) is an antibiotic anthracycline that is commonly used in chemotherapy for many solid tumors and leukemias,[11,12] and it also inhibits angiogenesis.[13] The efficacy of DOX is limited by its resistance mechanisms and toxic side effects, especially the irreversible damage caused by cardiotoxicity.[14] Increasing its efficacy and reducing its toxicity is necessary for its clinical use.

Sterically stabilized liposomes (SSL), also called stealth liposomes, can avoid phagocytosis by the reticuloendothelial system, leading to a prolonged in vivo circulation time for the drug loaded.[15] Also, a previous study demonstrates the advantage of PEGylated liposomes as the drug carrier for intravitreal administration, including slow drug release and protection of liposomes from degradation or leakage.[16]

In this paper, it was assumed that YSA-modified DOX-loaded stealth liposomes could increase the accumulation of drugs into CNV, enhance the intracellular uptake of drugs, and improve the therapy efficacy and reduce the toxicity of DOX as well. For the proof of concept, the YSA peptide was coupled to the PEGylated liposomes in this study, and the YSA-modified DOX-loaded stealth liposomes (YSA-SSL-DOX) were constructed and characterized using SSL-DOX as the control. A human RPE cell line (ARPE-19) was selected as a cell model to identify the specificity of YSA-SSL-DOX to RPE cells in vitro. A laser-induced CNV rat model was used to assess the efficacy of this active targeted delivery system, and its retinal toxicity was also investigated.

Materials and Methods

YSA peptide was obtained from ChinaPeptides (Shanghai, China). DOX was supplied by Zhejiang Hisun Pharmaceutical (Taizhou, China). Cholesterol (CHOL), polyethylene glycol–distearoylphostearoylphosphatitylethanolamine (DSPE-PEG$_{2000}$), and DSPE-PEG-NHS (1,2-dioleoyl-sn-glycero-3-phosphoethanolamine-n-[poly(ethyleneglycol)]-hydroxy succinamide, PEG Mw = 2000) were purchased from NOF (Tokyo, Japan). Hoechst 33258 and fluorescein-labeled dextran (FITC-

From the [1]Peking University Eye Center, Peking University Third Hospital, and the [2]State Key Laboratory of Natural and Biomimetic Drugs, School of Pharmaceutical Sciences, Peking University, Beijing, People's Republic of China.

Supported by projects from National Science Foundation (No. 81130059) and Ministry of Science and Technology of China (No. 2009CB930300 and No. 2009ZX09310-001).

Submitted for publication March 30, 2012; revised June 19, August 8, August 28, and September 11, 2012; accepted September 11, 2012.

Disclosure: **J. Wang**, None; **Y. Liu**, None; **Y. Li**, None; **W. Dai**, None; **Z. Guo**, None; **Z. Wang**, None; **Q. Zhang**, None

*Each of the following is a corresponding author: Yu-ling Liu, Peking University Eye Center, Peking University Third Hospital, 49 North Garden Road, Haidian District, Beijing 100191, People's Republic of China; yulingliu@medmail.com.cn.

Qiang Zhang, State Key Laboratory of Natural and Biomimetic Drugs, School of Pharmaceutical Sciences, Peking University, Beijing 100191, People's Republic of China; zqdodo@bjmu.edu.cn.

Investigative Ophthalmology & Visual Science, October 2012, Vol. 53, No. 11

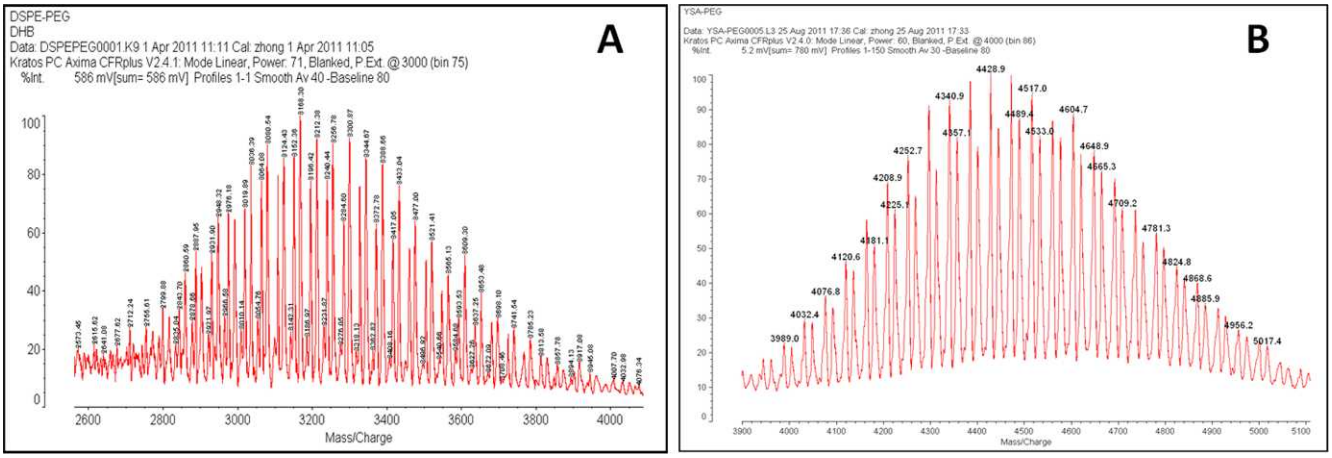

Figure 1. Mass spectrum of DSPE-PEG-NHS (**A**) and DSPE-PEG-YSA (**B**). The figures showed the successful conjugation of DSPE-PEG-YSA, and the conjugation molar ratio was 1:1. The product was composed of a series of compounds due to the different lengths of PEG groups.

Dextran, mW, 2×10^6) were supplied by Sigma-Aldrich (St. Louis, MO). Hydrogenated soy phosphatidylcholine (HSPC) was supplied by Lipoids GmbH (Hanover, DE). The dialysis bag (MWCO 3500) was supplied by JingKeHongDa Biotechnology Co., Ltd. (Beijing, China).

Conjugation of YSA to PEGylated Lipid

YSA and DSPE-PEG-NHS in the molar ratio of 1:2 were dissolved in dimethylformamide and reacted at room temperature in a pear-shaped flask with gentle stirring. Triethylamine was added to adjust pH to a slightly alkaline condition. The reaction was allowed to proceed for 48 hours and was traced by TLC until the spot of YSA disappeared completely. The reaction product was dialyzed against water for 3 days in order to remove all impurities and was then lyophilized. The formation of DSPE-PEG-YSA was identified by MALDI-TOF MS (AXIMA-XFR PlusX; Shimadzu, Kyoto, Japan).

Preparation and Characterization of Liposomes

Blank liposomes were prepared by a film dispersion method[17]: HSPC, CHOL, DSPE-PEG (20:10:2, molar ratio) for SSL and HSPC, CHOL, DSPE-PEG, DSPE-PEG-YSA (20:10:1.6:0.4) for YSA-SSL were dissolved in chloroform, which was later evaporated. Then the lipid film was hydrated with 123 mM ammonium sulfate, extruded through a 200-nm filter three times, and dialyzed against PBS. To prepare DOX liposomes, DOX was loaded into the blank liposomes using an ammonium sulfate gradient loading method.[18]

The particle size, polydispersity index (PDI), and zeta potential were monitored by the dynamic light scattering method using a Malvern Zetasizer (Nano ZS; Malvern Instruments, Worcestershire, UK). The morphology of YSA-SSL-DOX was investigated with a transmission electron microscope (JEM-200CX; JEOL, Tokyo, Japan).

Entrapment Efficiency of DOX in Liposomes

The encapsulation efficiency of DOX was estimated as in a previous report.[19] The supernatants were analyzed with a UV spectrophotometer (TU1901 spectrophotometer; Purkinje General Instrument Co., Ltd., Beijing, China).

In Vitro Leakage Studies

The leakage of drugs from liposomes was monitored by dialysis (MWCO 14000; JingKeHongDa Biotechnology Co., Ltd.) against PBS containing 1% hyaluronate sodium for 48 hours at 37°C. Aliquots of released medium were taken at different times and were immediately replaced with the same volume of fresh medium. Samples were analyzed for the released DOX, using the UV spectrophotometer at 485 nm. The linear response in UV absorption was found in the range of 0.5 to 40 μg/mL. From the total drug concentration of the liposome formulation, percentage released at each time point was calculated, and the obtained data were modeled with various mathematical models.

Stability Studies

Liposomes were stored at 4°C for up to 28 days under light protection. In predetermined time intervals, the appearance, particle size, and drug loading of liposomes were evaluated.

Cell Culture

A human RPE cell line (ARPE-19; American Type Culture Collection, Manassas, VA) was used at passages 12 to 16. The cells were routinely grown in 1:1 Dulbecco's modified Eagle medium/F12 with 10% fetal

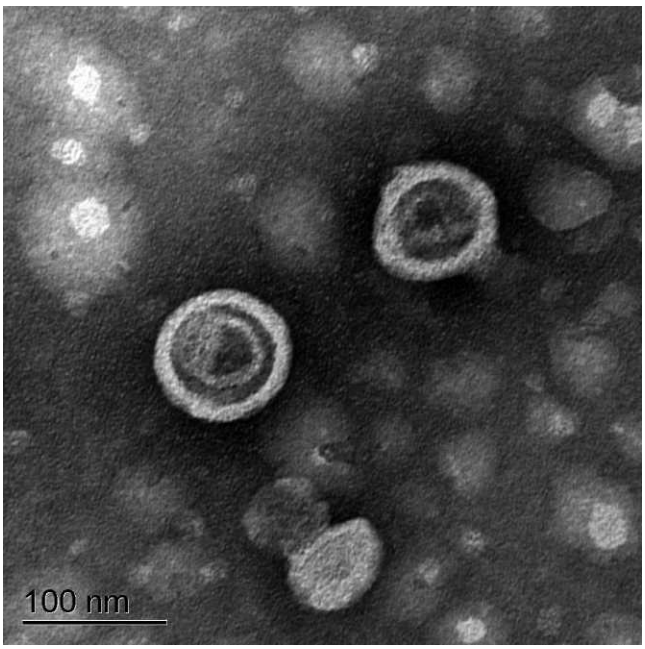

Figure 2. The morphology of YSA-SSL-DOX under a transmission electron microscope. The size of YSA-SSL-DOX was approximately 100 nm. *Bar* = 100 nm.

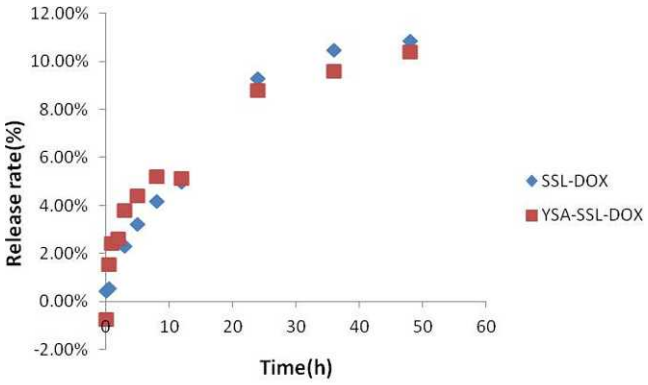

Cumulative release curves of fitting table

Sample	Fitting equation	Fitting results	R
SSL-DOX	Zero-order equation	Q=0.0022t+0.0184	0.9563
	First-order equation	Ln(1-Q)=-0.0024t-0.0183	0.9591
	Higuchi equation	Q=0.0166t^1/2-0.0004	0.9840
YSA-SSL-DOX	Zero-order equation	Q=0.002t+0.0234	0.9199
	First-order equation	Ln(1-Q)=-0.0021t-0.0236	0.9260
	Higuchi equation	Q=0.0153t^1/2+0.0051	0.9834

Figure 3. In vitro leakage of doxorubicin from YSA-SSL-DOX in comparison with that from SSL-DOX ($n = 3$) and cumulative release curves of both liposomes.

bovine serum and antibiotics (penicillin 100 U/mL, streptomycin 100 μg/mL). The cells were maintained at 37°C in an atmosphere containing 5% CO_2.

Flow Cytometry Analysis

ARPE-19 cells were seeded into six-well plates and cultured overnight at 37°C. After applying liposomes (20 μg/mL DOX), cells were further cultured for 3 hours. The drug-free culture medium was used as a blank control. The cells were washed three times with cold PBS (pH 7.4), and the fluorescence intensities of DOX in cells were examined by a FAScan flow cytometer (FACSCalibur; San Jose, Becton Dickinson, CA).

Confocal Microscopy Analysis

ARPE-19 cells were grown in chambered coverslips and incubated with liposomes (containing 20 μg/mL DOX) diluted in culture medium at 37°C for 3 hours. The cells were washed three times with PBS, fixed with 95% ethanol, and then treated with Hoechst 33258 for 15 minutes for nuclei staining. Fluorescent images of cells were analyzed using a TCS SP5 confocal microscope (excitation/emission: 480/540 nm; Leica, Heidelberg, Germany).

Expression of EphA2 Receptor on ARPE-19 Cells

ARPE-19 cells were grown on a glass-bottomed dish to 50% confluence and then washed three times with cold PBS and fixed in 4% paraformaldehyde for 15 minutes at room temperature. The cells were blocked with 1% BSA in 0.1 M PBS for 30 minutes, followed by incubation with the primary antibodies (1:100 dilution rat antihuman monoclonal EphA2; Abcam, Cambridge, MA) for 12 hours at 4°C.

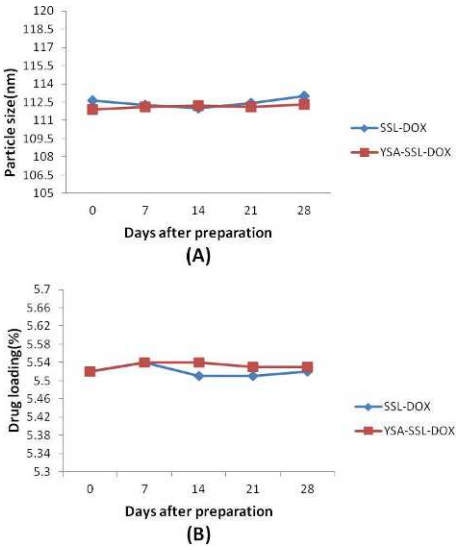

Figure 4. Stability study of liposomal dispersions stored at 4°C for 28 days. (**A**) Change of particle size. (**B**) Change of drug loading.

Negative controls (PBS added) were included. After washing, the cells were incubated with the secondary antibody (1:40 dilution TRITC-goat anti-rat IgG; Beijing Kang Wei Biotech, Beijing, China) for 45 minutes at 37°C and then treated with Hoechst 33258. Fluorescent images of cells were captured by laser scanning confocal microscopy.

Therapeutic Efficacy in Laser-Induced CNV in Rats

Brown Norway (BN) rats (Vital Laboratory Animal Center, Beijing, China) were treated in accordance with the recommendation of the ARVO Statement for the Use of Animals in Ophthalmic and Vision Research, with the approval of the Institutional Authority for Laboratory Animal Care. Briefly, male BN rats (180–220 g) were weighed and randomly divided into different treatment groups ($n = 3$, six eyes). Laser-induced CNV rats were prepared according to Liu's method.[20] The spots for laser treatment were located between major retinal vessels. Disruption of Bruch's membrance was confirmed by central bubble formation.[21]

In order to select the suitable dose of liposomal DOX, 1 day after laser photocoagulation, each group of rats ($n = 3$, six eyes) was intravitreously injected with normal saline (NS; 2.5 μL), SSL-DOX (1 μg/1 μL/eye), YSA-SSL-DOX (1 μg/1 μL/eye), SSL-DOX (2.5 μg/2.5 μL/eye), YSA-SSL-DOX (2.5 μg/2.5 μL/eye), SSL-DOX (5 μg/5 μL/eye), or YSA-SSL-DOX (5 μg/5 μL/eye). At the end of 2 weeks, rats under deep

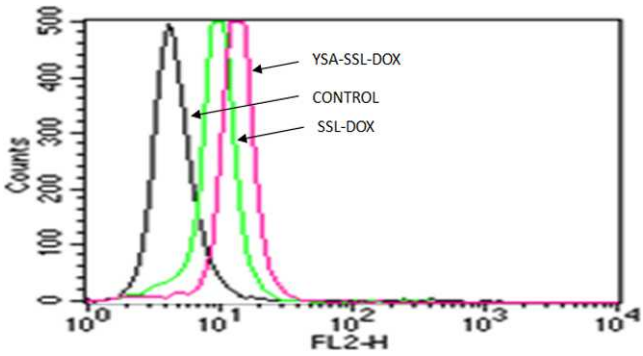

Figure 5. Flow cytometry measurement of doxorubicin uptake by ARPE-19 cells. ARPE-19 cells were incubated with SSL-DOX or YSA-SSL-DOX at 37°C for 3 hours. The concentration of doxorubicin was 20 μg/mL for all formulations.

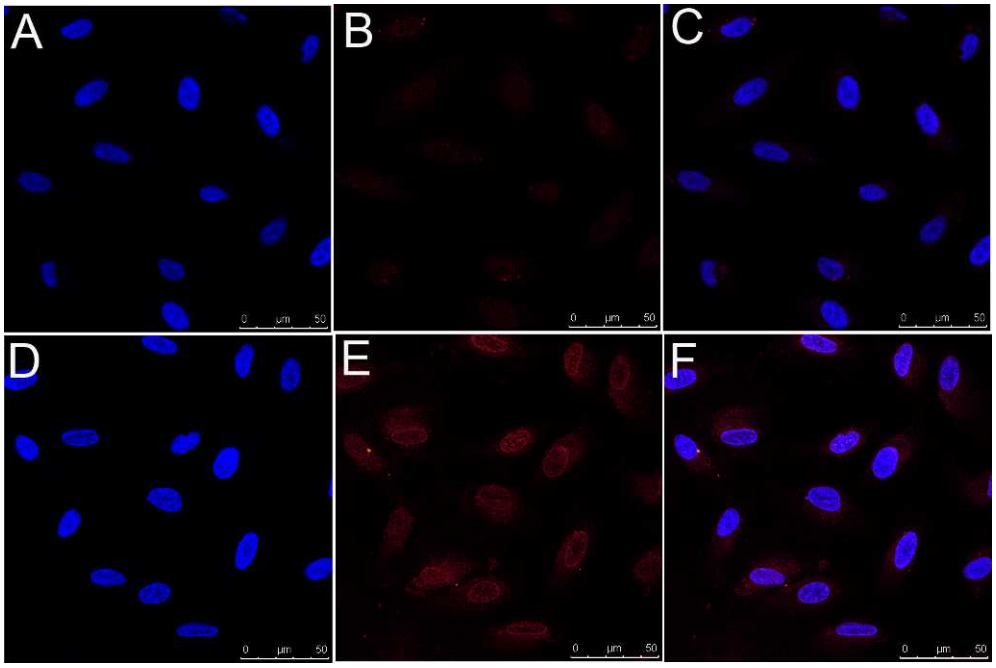

FIGURE 6. Confocal microscopy images of ARPE-19 cells incubated with SSL-DOX (**A–C**) and YSA-SSL-DOX (**D–F**) at 37°C for 3 hours. Doxorubicin concentration was 20 μg/mL. Cells were fixed and then treated with Hoechst 33258 for nuclei staining. *Red*: fluorescence of doxorubicin. *Blue*: fluorescence of Hoechst 33258. Colocalization (**C**, **F**) of Hoechst 33258 and doxorubicin was presented (the overlapped fluorescence of *blue* and *red*).

anesthesia were perfused with FITC-Dextran, and choroidal flat mounts were calculated using a method similar to that used in a previous report.[22] Elimination of burns that had not ruptured Bruch's membrane and caused a large hemorrhage resulted in the following number of rupture sites for analysis in each group ($n > 3$).

The CNV was observed by fluorescein fundus angiography (FFA) 1 and 2 weeks after intravitreous injections of different therapy groups. Briefly, the rats were anesthetized, and the pupils were dilated exactly as mentioned above. Then 2 mL of 10% sodium fluorescein was intraperitoneally injected in rats, and fluorescein fundus angiograms were obtained using Phoenix Research Laboratories MicronIII (American Health & Medical Supply International Corp., Pleasanton, NY).

Toxicity Study

The rats were divided into five groups, and normal BN rats were injected intravitreously in both eyes with YSA-SSL-DOX (with 1, 2.5, or 5 μg DOX), YSA-SSL, and NS, respectively. The rats were sacrificed 14 days after administration. The sections from the rat eyes were made, stained, and examined as usual.

Apoptosis was detected by the TUNEL method, according to the manufacturer's protocol (In Situ Cell Death Detection Kit, TMR red; Roche Applied Science, Mannheim, Germany).

Statistics

Statistical evaluations were performed using one-way ANOVA. A P value less than 0.05 was considered to be significant.

RESULTS

Conjugation of YSA to PEGylated Lipid

An activated DSPE-PEG (DSPE-PEG-NHS) was used to conjugate YSA to DSPE-PEG. The reaction takes place between α-amines of the YSA and NHS groups of the lipid. YSA was successfully covalently conjugated to DSPE-PEG-NHS with the molar ratio of 1:1 under the conditions of reaction (48 hours at room temperature, slightly alkaline, gentle stirring, and 1:2 molar ratio). The structures of DSPE-PEG-NHS and DSPE-PEG-YSA were confirmed by mass spectrometry (Fig. 1). The structure of DSPE-PEG-YSA was used to prepare YSA-SSL-DOX.

Characterization and Stability of Liposomes

The particle size, PDI, and zeta potential of SSL-DOX were 112.23 ± 2.10, 0.185 ± 0.054, and −1.705 ± 1.419 nm, respectively, while those of YSA-SSL-DOX were 112.60 ± 5.40, 0.188 ± 0.053, and −2.733 ± 1.157 nm, respectively. The encapsulation efficiency of DOX in both liposome systems was more than 95%. These data indicated that the modification of YSA did not significantly affect the characterization of SSL-DOX. In Figure 2, TEM confirmed that the particle size of YSA-SSL-DOX was approximately 100 nm. Besides, the membrane

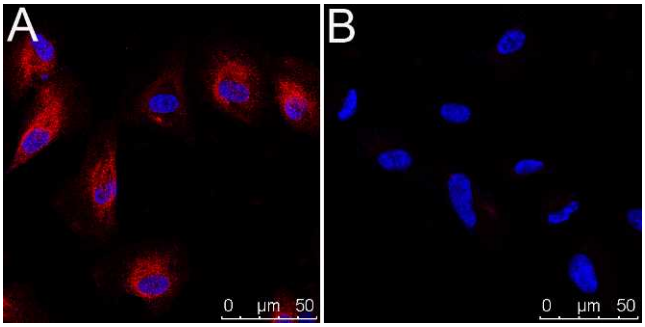

FIGURE 7. Expression of EphA2 on ARPE-19 cells. (**A**) Confocal microscopy images of EphA2 on ARPE-19 cells. *Red* represents the fluorescence of TRITC (secondary antibody conjugated). *Blue* represents fluorescence of Hoechst 33258. (**B**) Negative control (PBS added instead of primary antibodies).

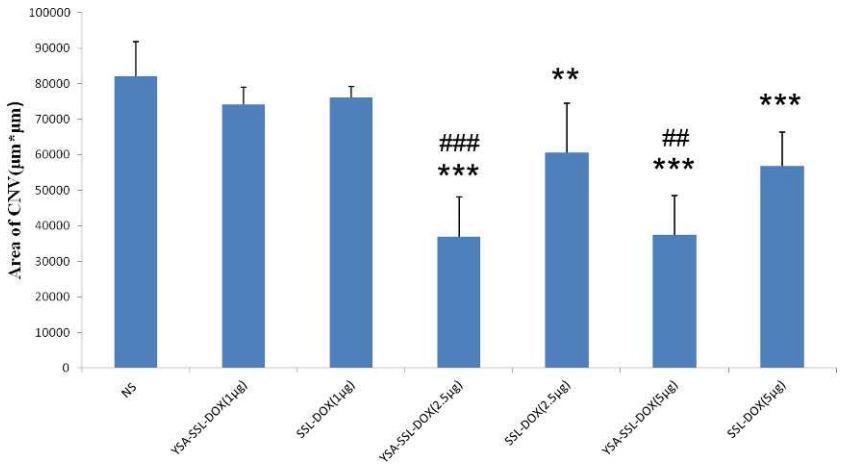

Figure 8. Quantitative evaluation of the choroidal flat mounts. The area of CNV was measured after treatment with different doxorubicin concentrations ($n > 3$). The data are presented as mean ± SD. $^{**}P < 0.01$, $^{***}P < 0.001$ versus NS; $\#\#P < 0.01$, $\#\#\#P < 0.001$ versus SSL-DOX with the same dose of DOX.

structure of this kind of liposome could be clearly seen in Figure 2.

In Vitro Leakage Studies of DOX from Liposomes

In vitro leakage studies of DOX from YSA-SSL-DOX and SSL-DOX at 37°C are shown in Figure 3. There was no significant difference in the release rate between these two liposome formulations ($P = 0.842$), again revealing the little effect from the peptide modification. Both exhibited a relatively slow release of DOX from liposomes under in vitro release conditions, suggesting little drug leakage from both liposomal DOX systems. The release rate of DOX at 3 hours from YSA-SSL-DOX or SSL-DOX was less than 4%, while this value was

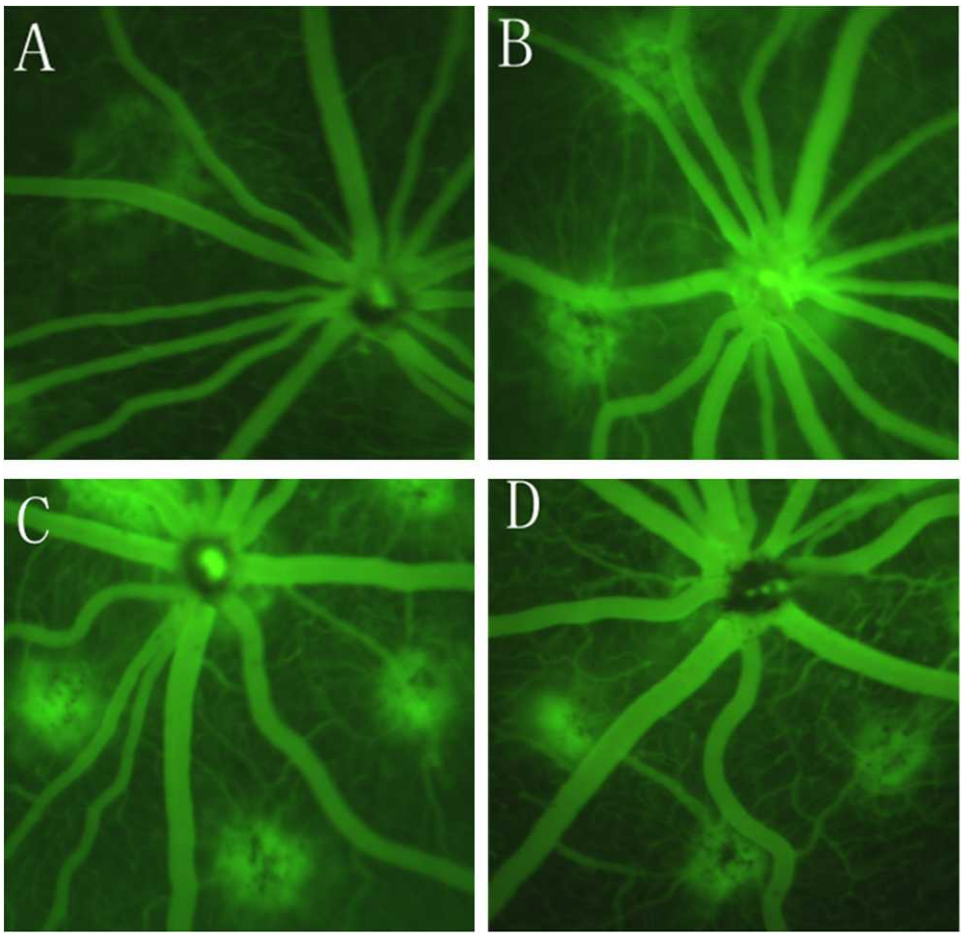

Figure 9. Laser-induced CNV on fluorescein angiogram. Representative images of CNV staining and leakage on fluorescein angiograms 2 weeks after intravitreous injection of NS (**A**), FREE-DOX (**B**), SSL-DOX (**C**), and YSA-SSL-DOX (**D**).

approximately 10% at 48 hours. Both of the release profiles were nonlinear during the test period, and the in vitro release curve was best fixed by the Higuchi equation compared to zero-order and first-order equations. The in vitro release model of YSA-SSL-DOX was

$$Q = 0.0153t^{1/2} + 0.0051 (R = 0.9834)$$

where Q represents cumulation release amount and t represents time, and the rate constant was 0.0153 ($hour^{-1}$).

According to this model, it takes approximately 176 days to release all drugs.

Stability Studies

Data on the stability of the liposomes stored at 4°C for 28 days are presented in Figure 4. It was noticed that there was little change in particle size and drug loading for the investigated liposomes. Also the physical appearance of the liposomal suspension did not change during this period of time.

Cellular Uptake of Liposomal DOX by Flow Cytometry Analysis

Figure 5 displays the cellular uptake of liposomal DOX in flow cytometry studies, which can provide quantitative data. It was found that cellular uptake of DOX in ARPE-19 cells was different between the two systems. The mean fluorescent intensity of DOX was 13.86 in the actively targeted group, much higher than that in the passively targeted group (10.76).

Intracellular Uptake and Distribution of Liposomal DOX by Confocal Scanning Analysis

Figure 6 illustrates the cellular uptake and distribution of DOX in ARPE-19 cells monitored by laser confocal scanning microscopy. As shown in Figure 6, greater DOX fluorescence intensity was observed in cells treated with YSA-SSL-DOX compared to those treated with SSL-DOX. This is in good accordance with the flow cytometry study. Additionally, besides some distribution in cytoplasm, the majority of the red fluorescence of DOX was found in the nuclear region, possibly due to the tropism of DOX to the cell nucleus. Up to now, our studies in cell level both demonstrated that the YSA peptide facilitated the intracellular endocytosis of DOX loaded in liposomes in the ARPE-19 cell line.

Expression of EphA2 Receptor on ARPE-19 Cells

The expression of EphA2 on ARPE-19 cells was demonstrated by confocal microscopy images as shown in Figure 7. This observation was important because it provided substantial evidence for the increased endocytosis of liposomal DOX by a receptor-mediated mechanism.

In Vivo Therapeutic Efficacy of CNV

The values of choroidal flat mounts observed after different treatments are shown in Figure 8. Except for the 1-μg liposome group, all of the treatment groups demonstrated significant efficacy in vivo compared to the NS group ($P < 0.01$). YSA-SSL-DOX groups (2.5 and 5 μg) showed an enhanced therapeutic effect compared to SSL-DOX groups (2.5 and 5 μg) ($P < 0.001$ or $P < 0.01$, respectively). There was no significant difference in CNV area between the 2.5- and 5-μg YSA-SSL-DOX groups, so we used the 2.5-μg group in the following test.

Figure 9 shows the representative images of CNV staining and the leakage on fluorescein angiograms 2 weeks after intravitreous injection of NS, free DOX, SSL-DOX, or YSA-SSL-DOX. It was indicated that there were obvious differences in CNV area and fluorescence leakage in FFA between the NS group and other therapy groups. Rats treated with YSA-SSL-DOX showed the least CNV area and fluorescence leakage in FFA.

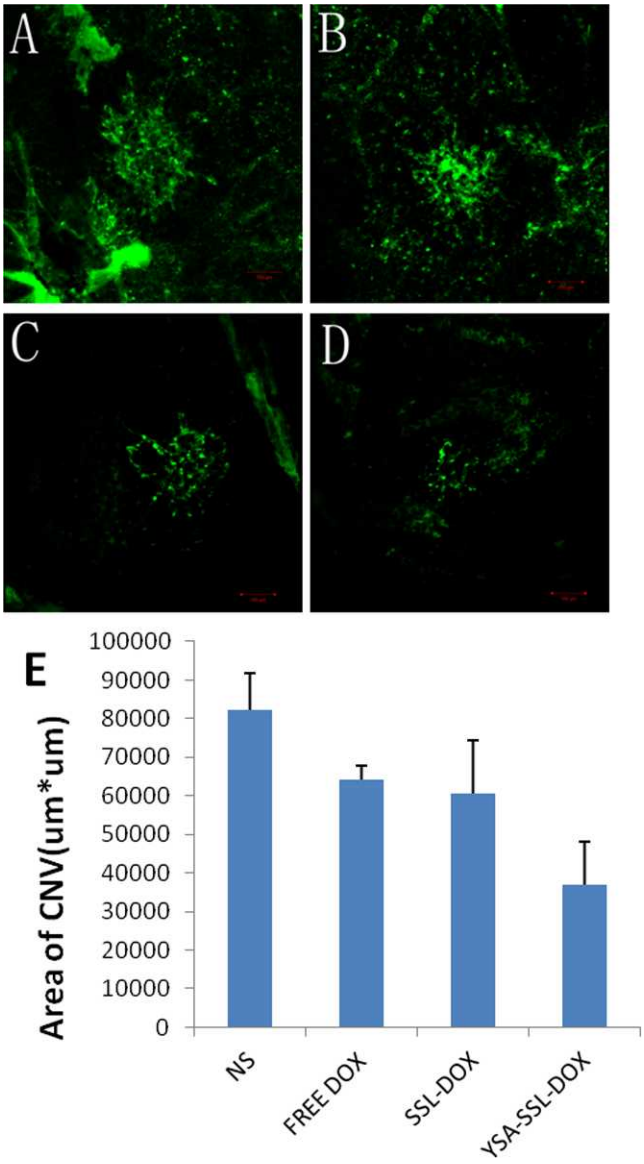

Figure 10. Effects of NS (**A**), FREE DOX (**B**), SSL-DOX (**C**), and YSA-SSL-DOX (**D**) on the size of the CNV complex. Representative choroidal flat mounts with FITC-dextran perfused vessels (*green*). (**E**) Quantification of the choroidal flat mounts. *Scale bar* = 100 μm. Data are reported as the mean ± SD.

Representative choroidal flat mounts are presented in Figure 10. Quantification of choroidal flat mounts is given in Figure 10E. The effects of NS, free DOX, SSL-DOX, and YSA-SSL-DOX on the size of the CNV complex were similar with those observed in Figure 9. Namely, all therapy groups significantly decreased the CNV area compared to the NS group, while YSA-SSL-DOX most reduced this value. The CNV area in the YSA-SSL-DOX group was significantly less than that in the SSL-DOX group.

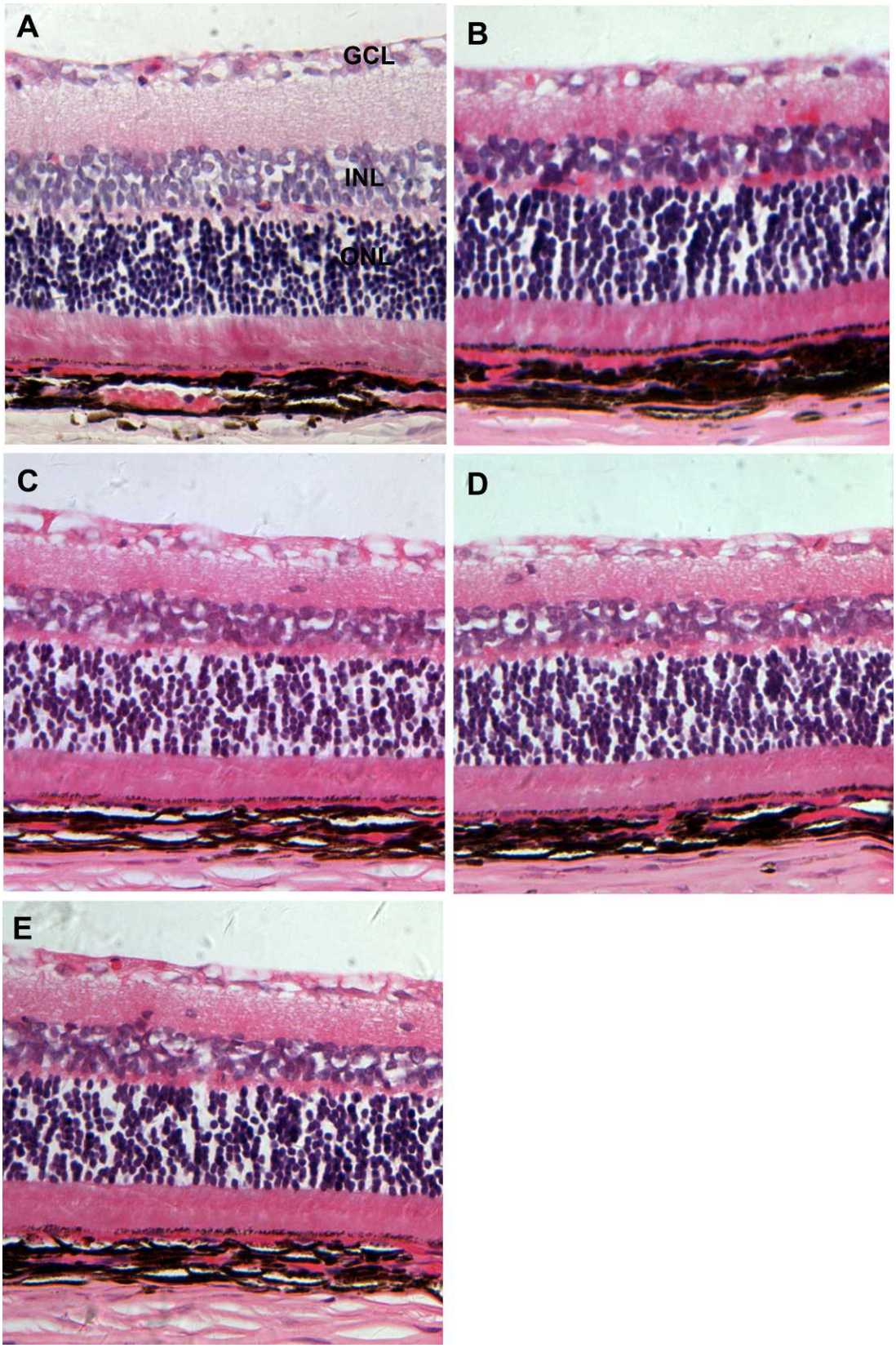

Figure 11. Effect of YSA-SSL-DOX on retinal structure in BN rats. Histological changes were evaluated 14 days after intravitreous injection of NS, YSA-SSL, and YSA-SSL-DOX (with 1, 2.5, 5 μg DOX). The sections were stained with hematoxylin and eosin. (**A**) NS; (**B**) YSA-SSL; (**C**) YSA-SSL-DOX (with 1 μg DOX); (**D**) YSA-SSL-DOX (with 2.5 μg DOX); (**E**) YSA-SSL-DOX (with 5 μg DOX). GCL, ganglion cell layer; INL, inner nuclear layer; ONL, outer nuclear layer. *Bar* = 100 μm.

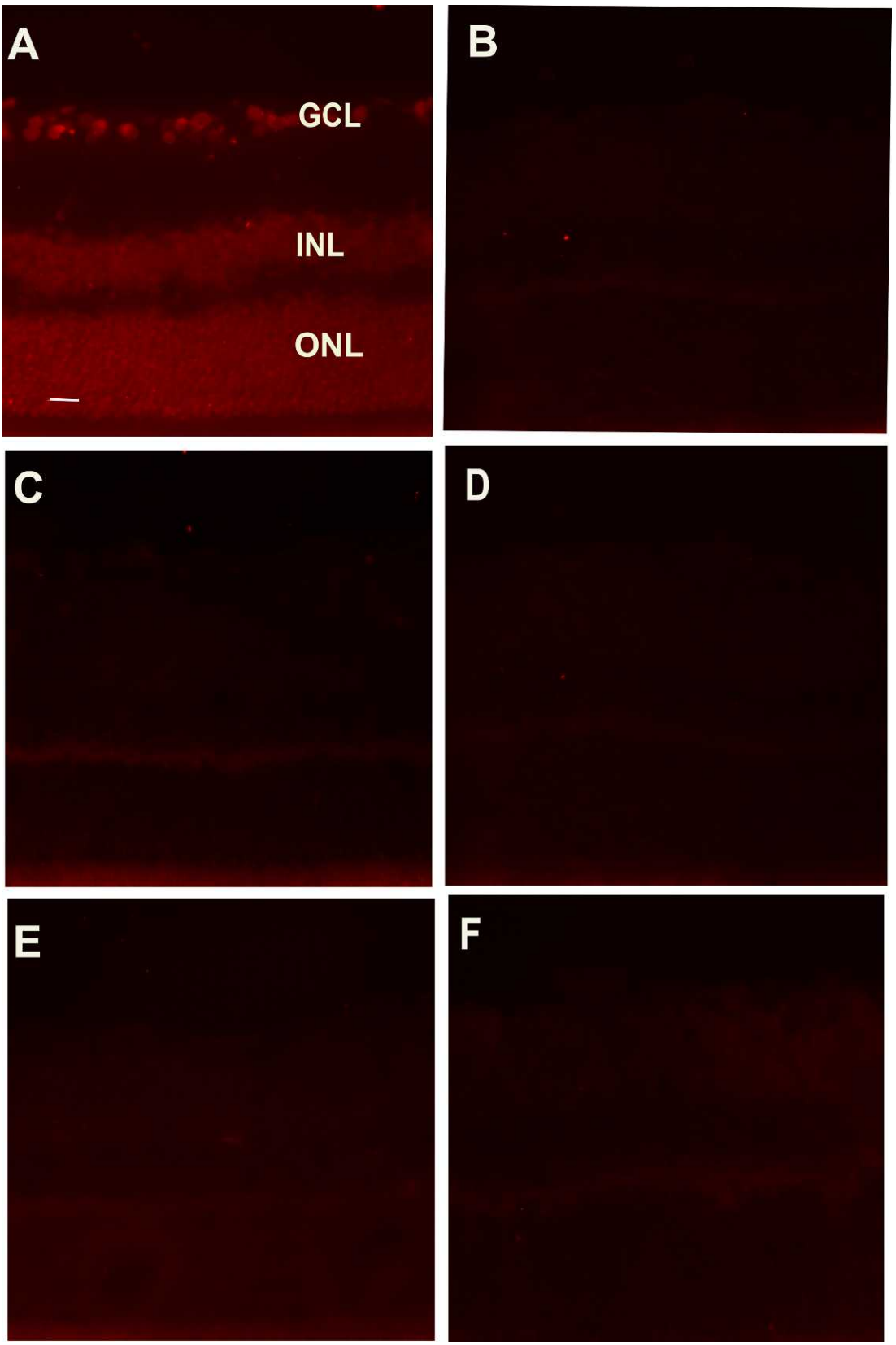

Figure 12. TUNEL assay for the rat retina treated with different amounts of YSA-SSL-DOX. (**A**) Positive control; (**B**) Negative control; (**C**) YSA-SSL; (**D**) YSA-SSL-DOX (1 μg DOX); (**E**) YSA-SSL-DOX (2.5 μg DOX); (**F**) YSA-SSL-DOX (5 μg DOX). *Bar* = 100 μm.

Histological Analysis

Fourteen days after intravitreal injection of YSA-SSL-DOX (with 1, 2.5, or 5 μg DOX), YSA-SSL, and NS, it was observed that the related tissues were clear, without inflammatory cells. The effect of YSA-SSL-DOX on retinal structure in BN rats is presented in Figure 11. Compared to the NS group, the ganglion cell layer, inner nuclear layer, and outer nuclear layer of rat retina were intact, without obvious damage in the groups of YSA-SSL and YSA-SSL-DOX with different doses of DOX. There was actually no significant difference among different groups. This study indicated the safety of both liposome systems to the rat eye, especially the retina, in the given doses and administration route.

Apoptosis Analysis of the Rat Retina

TUNEL assay of the rat retina with various liposome formulations (0, 1, 2.5, 5 μg DOX) is shown in Figure 12. In the positive control group, apoptosis could be clearly seen in the ganglion cell layer, inner nuclear layer, and outer nuclear layer of the rat retina. However, 14 days after intravitreal injection of YSA-SSL-DOX, it was demonstrated that the number of apoptosis cells was not significantly increased in each section of rat retina compared to the normal BN rat (negative control group) and YSA-SSL group. Together with the above histological analysis, it seems that the toxicity of YSA-SSL-DOX on the rat retina is low under the test conditions.

Discussion

According to our knowledge, this is the first time that the YSA peptide has been used to modify the stealth liposome that targets EphA2 in neovasculatures. The modification of YSA on the surface of liposomes was optimized in our study. As a result, higher cell uptake of YSA-SSL-DOX was observed when the molar ratio of DSPE-PEG:DSPE-PEG-YSA was 1.6:0.4, which was used in the final formulation.

SSL-DOX was prepared as the main control of YSA-SSL-DOX. It is important that the two liposome systems are very similar in their physicochemical properties. As mentioned above, this was true in our study. In this way, the major difference between these two lipid carriers was the modification of YSA, which is favorable for comparison with other studies.

Usually, positively charged particles are more effective in their interaction with a negatively charged cell membrane.[23] Here, both SSL-DOX and YSA-SSL-DOX are negatively charged and their surface potentials are very weak, so we think that the electrostatic force may not be the main interaction between liposomes and cells.

As shown in Figure 3, DOX was released from both liposome systems very slowly, less than 4% within 3 hours. In cell tests, the cellular uptake was conducted within 3 hours. Namely, most of the red fluorescence detected in flow cytometry profiles and confocal microscopy images might be that of liposomal DOX, but not the free DOX already released from liposomes.

In the in vivo study, the CNV area was recorded 14 days after laser photocoagulation, because at this time this value was usually the largest, being favorable for observation. Additionally, DOX was used as the positive control in the efficacy test. Although it showed some effect against CNV, its clinical use is almost impossible. It was reported previously that intravitreal administration of doxorubicin, likely caused by the oxygen radicals of DOX, was suspected for toxicity at the injection site, such as abnormality in the inner layer of the retina, especially to retinal ganglion cells.[24] Besides, there was a good correlation between the in vitro cell uptake and in vivo efficacy studies.

The development of an intravitreally injectable DOX carrier system could reduce its cytotoxicity and maintain a therapeutic level for a prolonged time. Moritera et al. prepared DOX microspheres and did not observe obvious toxicity after intravitreous injection of 10 μg to the rabbit eye.[25] As seen in Figures 11 and 12 in this study, there was no visible toxicity of YSA-SSL-DOX found on the rat retina. This might be attributed to the encapsulation of DOX in liposomes and also to the slow drug release. The elimination pathways of liposomes after intravitreal administration in rats were reported, and there was no adverse effect found to the eye in the short to medium term.[26]

Up to now, there have been no reports about the expression of EphA2 receptors in rat CNV. There are no choroidal cell lines available now, and the rationality of using primary choroidal cells is questionable because of the many treatments involved. In this study, we demonstrated for the first time the presence of EphA2 receptors on ARPE-19 cells, which have a close relationship in space with CNV. And the specific interaction between drug-loaded liposomes and RPE cells may be considerably helpful for drugs to concentrate in RPE cells and then diffuse into CNV. Our studies proved that EphA2 receptor-targeted liposomes were significantly superior to nontargeted liposomes in the treatment of rat CNV, indicating that EphA2 might be present on the choroidal cells. However, questions still remain to be explored in the future, such as the difference in expression of EphA2 receptors between rats and humans, and the correlation between the expression level of EphA2 receptors and stage of CNV.

In conclusion, we found that YSA-modified stealth liposomes could increase the intracellular delivery efficiency of drugs loaded in ARPE-19 cells and enhance the therapeutic efficacy against CNV in a rat model, while it showed only low toxicity on the rat retina. Therefore, it is suggested that EphA2 may play a role in CNV and that the EphA2 targeted drug delivery system, like YSA-SSL-DOX in this study, might improve the therapeutic efficacy against ocular angiogenesis disease such as diabetic retinopathy, corneal angiogenesis, and CNV.

References

1. Pascolini D, Mariotti SP, Pokharel GP, et al. 2002 Global update of available data on visual impairment: a compilation of population-based prevalence studies. *Ophthalmic Epidemiol*. 2004;11:67–115.
2. Ferrara N, Kerbel RS. Angiogenesis as a therapeutic target. *Nature*. 2005;438:967–974.
3. Bashshur ZF, Bazarbachi A, Schakal A, Haddad ZA, El Haibi CP, Noureddin BN. Intravitreal bevacizumab for the management of choroidal neovascularization in age-related macular degeneration. *Am J Ophthalmol*. 2006;142:141–143.
4. Ogawa K, Pasqualini R, Lindberg RA, Kain R, Freeman AL, Pasquale EB. The ephrin-A1 ligand and its receptor, EphA2, are expressed during tumor neovascularization. *Oncogene*. 2000; 19:6043–6052.
5. Cheng N, Brantley DM, Liu H, et al. Blockade of EphA2 receptor tyrosine kinase activation inhibits vascular endothelial cell growth factor-induced angiogenesis. *Mol Cancer Res*. 2002;1:2–11.
6. Chen J, Hicks D, Brantley-Sieders D, et al. Inhibition of retinal neovascularization by soluble EphA2 receptor. *Exp Eye Res*. 2006;82:664–673.
7. Pandey A, Shao H, Mark RM, Polverini PJ, Dixit VM. Role of B61, the ligand for the Eck receptor tyrosine kinase, in TNF-α-induced angiogenesis. *Science*. 1995;268:567–569.

8. Daniel TO, Stein E, Cerretti DP, St John PL, Robert B, Abrahamson DR. Elk and LERK-2 in developing kidney and microvascular endothelial assembly. *Kidney Int*. 1996; 57(suppl):S73–S81.
9. Flenniken AM, Gale NW, Yancopoulos GD, Wilkinson DG. Distinct and overlapping expression patterns of ligands for Eph-receptor tyrosine kinases during mouse embryogenesis. *Dev Biol*. 1996;179:382–401.
10. Koolpe M, Dail M, Pasquale EB. An ephrin mimetic peptide that selectively targets the EphA2 receptor. *J Biol Chem*. 2002; 277:46974–46979.
11. Berlin V, Haseltine WA. Reduction of adriamycin to a semiquinone-free radical by NADPH cytochrome P-450 reductase produces DNA cleavage in a reaction mediated by molecular oxygen. *J Biol Chem*. 1981;256:4747–4756.
12. Gilleron M, Marechal X, Montaigre D, Franczak J, Neviere R, Lancel S. NADPH oxidases participate to doxorubicin-induced cardiac myocyte apoptosis. *Biochem Biophys Res Commun*. 2009;388:727–731.
13. Zhang LL, Yu DY, Hicklin DJ, Hannay JA, Ellis LM, Pollock RE. Combined anti-fetal liver kinase 1 monoclonal antibody and continuous low-dose doxorubicin inhibits angiogenesis and growth of human soft tissue sarcoma xenografts by induction of endothelial cell apoptosis. *Cancer Res*. 2002;62:2034–2042.
14. Colombo T, Donelli MG, Urso R, Dallarda S, Bartosek I, Guaitani A. Doxorubicin toxicity and pharmacokinetics in old and young rats. *Exp Gerontol*. 1989;24:159–171.
15. Maruyama K, Ishida O, Takizawa T, Moribe K. Possibility of active targeting to tumor tissue with liposomes. *Adv Drug Deliver Rev*. 1999;40:89–102.
16. Bochot A, Fattal E, Boutet V, et al. Intravitreal delivery of oligonucleotides by sterically stability liposomes. *Invest Ophthalmol Vis Sci*. 2002;43:253–259.
17. Xiong XB, Huang Y, Lu WL, Zhang H, Zhang X, Zhang Q. Enhanced intracellular uptake of sterically stabilized liposomal doxorubicin in vitro resulting in improved antitumor activity in vivo. *Pharm Res*. 2005;22:933–939.
18. Harrigan PR, Wang KF, Redelmeier TE, Wheeler JJ, Cullis PR. Accumulation of doxorubicin and other lipophilic amines into large unilamellar vesicles in response to transmembrane pH gradients. *Biochim Biophys Acta*. 1993;1149:329–338.
19. Ying X, Wen H, Lu WL, et al. Dual-targeting daunorubicin liposomes improve the therapeutic efficacy of brain glioma in animals. *J. Controlled Release*. 2010;141:183–192.
20. Liu HA, Liu YL, Ma ZZ, Wang JC, Zhang Q. A lipid nanoparticle system improves siRNA efficacy in RPE cells and a laser-induced murine CNV model. *Invest Ophthalmol Vis Sci*. 2011; 52:4789–4794.
21. Campos M, Amara J, Becerra SP, Fariss RN. A novel imaging technique for experimental choroidal neovascularization. *Invest Ophthalmol Vis Sci*. 2006;47:5163–5170.
22. Edelman JL, Castro MR. Quantitative image analysis of laser-induced choroidal neovascularization in rat. *Exp Eye Res*. 2000;71:523–533.
23. Verma A, Stellacci F. Effect of surface properties on nanoparticle-cell interactions. *Small*. 2010;6:12–21.
24. Hu T, Le QH, Wu ZY, Wu W. Determination of doxorubicin in rabbit ocular tissues and pharmacokinetics after intravitreal injection of a single dose of doxorubicin-loaded poly-β-hydroxybutyrate microspheres. *J Pharm Biomed Anal*. 2007;43:263–269.
25. Moritera T, Ogura Y, Yoshimura N, et al. Biodegradable microspheres containing adriamycin in the treatment of proliferative vitreoretinopathy. *Invest Ophthalmol Vis Sci*. 1992;33:3125–3130.
26. Bochot A, Fattal E. Liposomes for intravitreal drug delivery: a state of the art. *J Controlled Release*. 2012;161:628–634.